Evidence for disease and antipsychotic medication effects in post-mortem brain from schizophrenia patients

Sabine Bahn, Man Kuan Chan, Laura Harris, Paul Guest, Tsz Tsang, Elaine Holmes

Evidence for disease and antipsychotic medication effects in *post-mortem* brain from schizophrenia patients

Running title: Disease and medication effects in schizophrenia brain

Man K. Chan[1], Tsz M. Tsang[2], Laura W. Harris[1], Paul Guest[1], Elaine Holmes[2], Sabine Bahn[#]

[1]Institute of Biotechnology, Department of Chemical Engineering and Biotechnology, University of Cambridge, Cambridge, UK

[2]Biomolecular Medicine, Department of Surgery and Cancer, Faculty of Medicine, Imperial College, London, UK

[#]Correspondence: Dr. Sabine Bahn MD PhD MRC Psych, Institute of Biotechnology, Department of Chemical Engineering and Biotechnology, University of Cambridge, Cambridge, CB2 1QT, UK. E-mail: sb209@cam.ac.uk. Tel: +44 1223 334151. Fax: +44 1223 334162.

Abstract

Extensive research has been conducted on *post-mortem* brain tissue in schizophrenia, particularly the dorsolateral prefrontal cortex (DLPFC). However, to what extent the reported changes are due to the disorder itself and which are the cumulative effects of lifetime medication remains to be determined. In this study, we employed label-free liquid chromatography-mass spectrometry (LC-MS^E) based proteomic and proton nuclear magnetic resonance (^{1}H NMR) based metabonomic profiling approaches to investigate DLPFC tissue from two cohorts of schizophrenia patients grouped according to their lifetime antipsychotic dose, together with tissue from bipolar disorder subjects, and normal controls (n=10 per group). Both techniques showed profound changes in tissue from low-cumulative-medication schizophrenia subjects, but few changes in tissue from medium-cumulative-medication subjects. Protein expression changes were validated by Western blot and investigated further in a third group of subjects who were subjected to high-cumulative-medication over the course of their lifetime. Furthermore, key protein expression and metabolite level changes correlated significantly with lifetime antipsychotic dose. This suggests that the detected changes are present prior to antipsychotic therapy and moreover, may be normalized with treatment. Overall, our analyses revealed novel protein and metabolite changes in low-cumulative-medication subjects associated with synaptogenesis, neuritic dynamics, presynaptic vesicle cycling, amino acid and glutamine metabolism, and energy buffering systems. Most of these markers were altered specifically in schizophrenia as determined by analysis of the same brain region from bipolar disorder patients.

Keywords: *post-mortem* brain; schizophrenia; antipsychotic medication; bipolar disorder; LC-MS^E; ^{1}H NMR.

Introduction

Schizophrenia (SCZ) is a debilitating psychiatric disorder that affects approximately 1% of the world population (1). Extensive research has been conducted to investigate brain regions such as the dorsolateral prefrontal cortex (DLPFC) since this area is thought to represent the primary site of higher cognitive function impairment (2). For example, cytoarchitectural, neurochemical (3) and structural (4) abnormalities have been observed in this brain region of SCZ patients, such as decreased neuronal size and dendritic spine density (5-8). Evidence in favour of abnormal neurotransmission, signal transduction (9), neural connectivity, GABAergic (10) and glutamatergic activity (11) has also been demonstrated in the DLPFC of these patients. There has been increasing interest in employing global protein profiling methodologies, including mass spectrometry (MS)-based methods, to examine the DLPFC of SCZ patients (12-20). Converging results from these studies have supported the case for synaptic, oxidative stress mitochondrial and metabolic dysfunction in the disorder. In support of this, the recent application of state-of-the-art metabonomic platforms and informatics tools have identified alterations in markers of energy and neurotransmitter metabolism in sub-regions of the DLPFC of SCZ patients (17, 21), and in animal models of antipsychotic drug treatment (22). However, most global profiling studies using *post-mortem* brain tissue have been performed on subjects who have been treated with varying lifetime antipsychotic medication doses. Although the confounding effects of factors such as *post-mortem* interval and tissue pH have been investigated in molecular profiling studies (23-26), those associated with cumulative lifetime antipsychotic doses have not been addressed fully. This is likely to be an important factor since neuroimaging analyses of SCZ subjects have demonstrated a correlation between cumulative antipsychotic dose and specific anatomical and cellular alterations (27, 28). With this in mind, we have attempted to identify the molecular signatures associated with the inherent pathological processes as well as antipsychotic drug-induced changes in DLPFC tissue from SCZ subjects who had received different cumulative lifetime antipsychotic doses. We conducted a parallel profiling study using label-free LC-MS^E based proteomic and ^1H NMR spectroscopy based metabonomic approaches. We also included DLPFC tissue from bipolar disorder (BPD) subjects in the analysis, to determine the specificity of any observed biomarkers for SCZ given that there is an aetiological overlap between SCZ and BPD and, epidemiological and genetic linkage studies have also identified a number of shared susceptibility loci between these two disorders (29).

Materials and methods

Tissue samples

Sixty *post-mortem* DLPFC Broadmann Area 9 (BA9) gray matter samples were obtained from the Stanley Medical Research Institute (Bethesda, MD, USA). The average fluphenazine mg equivalent (FME) was used as an indicator of cumulative lifetime antipsychotic dose (30). SCZ samples were separated into three demographically-matched groups according to FME: Group 1) low-cumulative-medication [(L-SCZ), FME: 6515±6465, n=10 (including 2 drug-naive with FME=0 and 2 with FME≤600)], Group 2) medium-cumulative-medication [(M-SCZ), FME: 86200±47499, n=10], and Group 3) high-cumulative-medication [(H-SCZ), FME: 182500±123855, n=10]. The medication groups were chosen, to the best possible, to give balanced groups with the maximum number of patients in each group with the least overlap in FME dose. The mean FME dose between the medication groups was significantly different (p=0.0005). In addition, 10 bipolar disorder (BPD) and 10 control (CT) subjects were matched and analysed. An additional batch of 10 controls was matched specifically to H-SCZ subjects as the latter was not matched to the previous control group with respect to gender. Unless stated otherwise, samples were matched for *post-mortem* brain interval (PMI), pH, age of onset, age of death, duration of illness and gender (summary of demographic details and statistical values are shown in Table 1; additional details are provided in Supplementary Tables S1 and S2). Samples from H-SCZ patients and matched controls were used for Western blot validation analyses only. Since the average brain pH of H-SCZ patients was significantly lower than that of the controls, Pearson correlation analyses were performed using GraphPad PRISM v5 (San Diego California, USA) to confirm that there were no effects of pH on protein expression (average r of -0.40 and 0.34, p>0.05). Approximately 70 mg of tissues were sectioned (15µm slices) using a Leica Cryostat tissue sectioning device (Milton Keynes, UK), collected into pre-chilled lysing matrix D tubes (MP Biomedicals, UK) and stored at -80ºC until use.

(Table 1 here)

Experimental design

Fractionation of *post-mortem* DLPFC tissue (n=60) from all subject groups (Table 1) was performed to increase proteome coverage of membrane-associated proteins. In the first stage of this study, membrane protein fractions from L-SCZ, M-SCZ, BPD and controls were analysed by LC-MS^E. In the next stage, differentially expressed proteins were validated by Western Blot analysis using membrane and soluble fractions, and unfractionated total brain lysate samples across all 5 groups [L-SCZ, M-SCZ, H-SCZ, BPD and controls]. In the final stage, ^{1}H NMR spectroscopy metabonomic analysis was carried out for L-SCZ, M-SCZ and controls. The same analysis for BPD samples from this brain collection was conducted previously (31).

Subcellular proteome fractionation and protein purification/digestion

Brain tissue sections were processed using the Subcellular Proteome Extraction Kit (Merck; Nottingham, UK) as described previously (32-34). Briefly, tissues were homogenized in 1mL ice cold Extraction Buffer I containing 5µL Protease Inhibitor Cocktail (PI) at 4°C using the FastPrep FP120 cell disrupter (Qbiogene; Cambridge, UK) set at speed 4 for 5 seconds. Homogenates were incubated on a rotary shaker for 30 minutes at 4°C and centrifuged at 11000g for 10 minutes. The supernatants (fraction I, enriched soluble proteins) were collected and pellets were suspended in 1mL of ice cold Extraction Buffer II containing 5µL PI by first flicking the tubes and then mixing on a rotary shaker for 60 minutes at 4°C. Following centrifugation at 6000g for 10 minutes, the supernatants (fraction II, enriched membrane proteins) were collected. Approximately 200µg of proteins from fraction II were precipitated using the ProteoExtract® Protein Precipitation Kit (Merck), reduced, alkylated and digested using the all-in-one trypsin digestion kit (MERCK). Trypsin was obtained from Promega (Madison, WI, USA).

LC-MS^E analysis

LC-MS^E was carried out and the reproducibility and quantitative reliability was assessed as described previously (35). To minimize systematic batch effects, sample preparation and MS acquisition were performed in a randomized order. The PLGS2.3 software was used for ion detection and clustering (36-39) and the embedded ion accounting algorithm employed for searching the *H. Sapiens* complete proteome fasta

sequence Integr8 database (http://www.ebi.ac.uk/integr8/FtpSearch.do?orgProteome Id=25; version 25), appended with S.cerevisiae enolase sequence (P00924). Data were normalized using the Trackstats software (Waters; Milford MA, USA) and filtered for replication using R (www.r-project.org) with criteria described previously (35). To perform quantitation on the protein level, peptide correlation analyses ($r>0.5$) were performed for every detected protein (35, 40). To identify significant alterations in protein expression levels between different experimental groups, 2-tailed Student's t-tests were performed ($p\leq0.05$) and false discovery rates (FDR) were calculated using the Benjamini & Hochberg correction approach (41). This approach calculates the proportion of statistically significant differences that are actually false positives. Biological process grouping was carried out using the Human Protein Reference Database (HPRD; http://www.hprd.org/) and the Database for Annotation, Visualization and Integrated Discovery (DAVID; http://david.abcc.ncifcrf.gov/).

Western blot analysis

Protein samples (10µg) were resolved on 4–12% NuPAGE Novex Bis-Tris gels (Invitrogen, Paisley, UK) and transferred electrophoretically onto nitrocellulose membranes. Membranes were washed three times for 5 minutes in phosphate buffered saline containing 0.1% Tween-20 (PBS-T) followed by incubation for 1 hour in Odyssey blocking buffer (LI-COR Biosciences; Cambridge, UK) and then overnight at 4ºC with primary antibodies diluted in the same buffer containing 0.1% Tween-20 (OBB-T) (details of the primary antibodies are shown in the legend for Figure 2a and Supplementary Figure S1). Membranes were washed five times 20 minutes in PBS-T followed by incubation with the appropriate infrared dye-linked secondary antibodies (800CW goat anti-mouse, 680CW goat anti-rabbit and 800CW goat anti-rat; Licor Biosciences) in OBB-T in the dark. Images were acquired using the Odyssey Infrared Imaging System and analysed and quantified using the Odyssey v3.0 Software. Calmodulin was used as internal control for normalizing protein loading differences as this protein showed no significant differences in abundance between disease and control by LC-MS^E [L-SCZ ($p=0.75$), M-SCZ ($p=0.80$), BPD: ($p=0.28$) and Western blot analysis (Figure 2b). For validation purposes, 2-tailed Student's t-tests were conducted and significance was regarded as $p<0.05$. Fold changes were calculated by dividing the average integrated intensity readings of disease by control samples.

^{1}H NMR spectroscopy

Separate tissue slices obtained from the same *post-mortem* brain specimens used in the above studies were homogenized while frozen in 1mL of methanol:deionised water (1:1) in 2mL microfuge tubes (Eppendorf; Loughborough, UK) containing a metal bead (Qiagen; West Sussex, UK), using a tissue grinder (Qiagen) set at 30 cycles/second for 5minutes. Chloroform (1mL) was added to produce aqueous and lipid phases. Homogenates were vortexed and centrifuged at 1200g for approximately 7 minutes at 5°C. The upper aqueous phase containing hydrophilic metabolites was collected and left to dry overnight at room temperature to remove methanol before freeze drying. Samples were reconstituted in 700µL of deuterium oxide (D_2O) and 600µL was transferred into NMR tubes for analysis. D_2O provides deuterium field frequency lock for the NMR spectrometer. ^{1}H NMR spectra were generated at 600.13 MHz on a Bruker DRX-600 spectrometer (Bruker Avance, Bruker GmBH; Rheinstetten, Germany) as described previously (31). Complete spectra (chemical shift range 0-10ppm) were processed using the Topspin v2.0 software (Bruker). Spectra were phase and baseline corrected and calibrated using the reference resonances of the CH_3 lactate doublet (1.33ppm). Any variation effect due to pre-saturation of water was removed by zeroing intensity values between 4.5 and 4.9ppm. To account for concentration differences between samples, data were normalized to the total integrated peak area intensity by converting the integral values into a percentage of the sum of the integral.

Chemometric modelling and interpretation of the ^{1}H NMR data

To identify metabolites differentiating disease and control groups, partial least squares discriminant analysis (PLS-DA) was performed on full resolution ^{1}H NMR spectral data using SIMCA P v12 (Umetrics AB; Umeå, Sweden). To remove confounding variation, orthogonal-projection to latent structures discriminant analysis (OPLS-DA) was used to model the data using MATLAB v6.5 (The Mathworks Inc, Natick; MA, USA) scripts proprietary to Imperial College London. This method represents an improvement to the traditional supervised PLS algorithm and enhances the interpretability of spectral variation between classes (42, 43). To confirm the differences identified by these multivariate analyses, univariate analyses (Wilcoxon-Mann-Whitney U tests (44)) were performed using GraphPad Prism v5. Significance was regarded as $p<0.05$ and fold changes were obtained by calculating the ratio between disease and control groups.

Results

Quality control

Membrane protein enrichment efficiency in fraction II was demonstrated by Western blot analysis of a DLPFC specimen using subcellular distribution markers. LC-MS^E analysis resulted in the identification of 370 proteins in fraction I and 568 proteins in fraction II. Fractionation efficiency, as evaluated by analysis of cellular distribution of these proteins, was demonstrated by identification of a higher proportion of soluble and membrane proteins in fractions I and II, respectively (details are provided in Supplementary Figure S1).

Mass Spectrometry

Quantitative analysis of fraction II resulted in identification of approximately 30 differentially expressed proteins ($p \leq 0.05$) out of the approximate 500 identifiable proteins in L-SCZ and BPD patients, compared to the control group (Figure 1). None of the differentially expressed proteins overlapped across the diseases. No significant changes were observed for the M-SCZ patients compared to the same control group. Differentially expressed proteins were assigned to biological process groups using HPRD and DAVID (Table 2 for L-SCZ and Supplementary Table S3 for BPD). Table 2 also indicates markers which have been reported previously in the literature in association with proteomic or transcriptomic analyses of SCZ DLPFC tissue, thereby providing an additional means of validation as many directions of change reported in the literature agree with our findings.

(Figure 1 and Table 2 here)

Western blot validation

Confirmation of mass spectrometry profiling results: Raw p-values for LC-MS^E data were corrected for multiple hypothesis testing using the Benjamini-Hochberg false discovery rate method (Table 2). As corrected p-values for differentially expressed proteins were relatively high, Western blot analyses were conducted to confirm changes in L-SCZ and BPD membrane fraction samples. Calmodulin was used as a loading control since this protein was not changed in this study, as determined by LC-MS^E and Western blot analyses. Antibodies were selected against 7 proteins to represent different functional networks and

directional changes in L-SCZ and BPD subjects. These included MAG, MARCKS, NCAM, GAP43 and NFM. Neuronal nitric oxide synthase (nNOS) was also examined due to its regulatory action on NCAM (45) and functional relevance in SCZ (46, 47). β-tubulinIII (TUBB) was tested as an example of a protein altered in BPD patients. Western blot analysis validated the expression changes in these proteins, with the exception of MAG (Figure 2a and 2b). The predicted change in nNOS was also confirmed in L-SCZ. These results confirmed the reliability of the label-free LC-MS^E based profiling approach. Validation was also conducted using soluble fractions and unfractionated total brain lysates from the L-SCZ patient samples. Overall, most of the changes identified in the membrane fractions were confirmed in the corresponding soluble fractions and total brain lysates (Figure 2b).

(Figure 2 here)

Assessment of disease specificity and effects of lifetime antipsychotic medication in schizophrenia: LC-MS^E analysis revealed that none of the differentially expressed proteins identified in samples from L-SCZ subjects were found in those from M-SCZ subjects. This was also confirmed by Western blot analyses of membrane fractions from L-SCZ, M-SCZ, H-SCZ and CT samples (Figure 2a and 2b). Overall, the results confirmed that the levels of MARCKS, GAP43 and nNOS were changed in L-SCZ but not in M-SCZ and H-SCZ. This suggested that abnormal expression of these proteins may be a primary disease change and not a medication effect. However, NFM did not show a clear pattern of expression relating to medication. NCAM was increased significantly in all SCZ medication groups and in BPD samples. This suggested that NCAM expression may not be affected by lifetime antipsychotic levels or mood stabilizer treatment and that it is not specific to SCZ. The LC-MS^E results showed no overlap in the differentially expressed protein profiles of SCZ and BPD subjects (Table 2 and Supplementary Table S3), as confirmed by Western blot analysis (Figure 2b). Biological process grouping using HPRD and DAVID also showed no overlap (Figure 1). The most notable changes for SCZ were 15 differentially expressed proteins involved in cell communication and 7 metabolism proteins, whereas BPD was marked by alterations of 8 cell communication proteins and 7 cell growth proteins (Figure 1).

Correlation analysis

The LC-MS^E profiling results showed changes in tissues from L-SCZ subjects but not in M-SCZ individuals. This suggests that these changes are associated with the primary disease state and, moreover, may be normalized with treatment. For this to be the case, expression changes should not only show a group difference according to treatment level, but also a direct relationship to lifetime antipsychotic dose within the group. In order to further investigate this possibility, FME and Western blot expression values from individual SCZ subjects were tested in correlation analyses. GAP43 (r=-0.77, p=0.025), MARCKS (r=-0.76, p=0.029) and, nNOS (r=-0.90, p=0.006) expression levels were significantly negatively correlated with FME, consistent with their identification as differentially expressed proteins in the L-SCZ group and their lack of change after more extensive drug treatment comprising the M-SCZ group (Supplementary Figure S2a). NCAM (r=0.64, p=0.085), on the other hand, was not significantly correlated with FME, consistent with the Western blot finding that this protein was altered in both the L-SCZ and the M-SCZ groups. The effects of lifetime antipsychotic dose were further confirmed by demonstrating a significant correlation between FME dose and levels of significantly altered metabolites [e.g. alanine (r=0.64, p=0.003) and branched amino acids (r=48, p=0.039)]. Similar to the case of NCAM, glutamine levels (r=-0.15, p=0.55) were also not significantly correlated with FME dose, as it was altered in both medication groups (Supplementary Figure S2b). We also considered the possibility that the molecular alterations may be confounded by a shorter duration of illness in patients with low FME. Although this factor was well matched between the L-SCZ and M-SCZ groups (p=0.27), the mean duration of illness was higher in H-SCZ patients which were investigated separately. Correlation analyses show that duration of illness did not affect expression of key validated proteins or levels of significantly altered metabolites (Supplementary Figure S3).

^{1}H NMR spectroscopy data analysis

PLS-DA of ^{1}H NMR spectroscopy data revealed a separation between the L-SCZ or M-SCZ and CT groups. O-PLS-DA showed the metabolites that are most influential to these separations (Figure 3a). Specifically, branched amino acids, alanine, creatine and glutamine were altered in L-SCZ patients. Most of the metabolites identified using multivariate analyses were confirmed by univariate statistical analysis (Figure 3b). Of the 4 metabolites altered in L-SCZ, 3 (branched chain amino acids, alanine and creatine) were not

changed in M-SCZ and only glutamine was changed in both groups. In addition, taurine was altered in M-SCZ but not in L-SCZ.

(Figure 3 here)

Discussion

This is the first study employing label-free LC-MS^E proteomic and ^1H NMR metabonomic profiling platforms to examine molecular effects of cumulative lifetime antipsychotic medication dose in *post-mortem* brain tissue (dorsolateral prefrontal cortex, BA9, gray matter) of SCZ patients. To control for non-specific effects of chronic psychiatric illnesses, the proteomic profile of BPD patients was also investigated to demonstrate that the changes reported are relatively specific for SCZ. Lifetime antipsychotic medication was found to have an effect on a number of proteins and metabolites in SCZ patients. The specificity of the protein expression changes identified in L-SCZ patients was also demonstrated relative to BPD providing evidence for diverging pathologies between the two disorders.

Disease signatures of schizophrenia and targets of drug effects

Out of the approximately 500 proteins and 16-20 metabolites identified per dataset, 34 proteins and 4 metabolites were altered in L-SCZ patients and only 1 protein (NCAM) and 2 metabolites (glutamate and taurine) were altered in M-SCZ patients. This suggested that a higher cumulative lifetime antipsychotic dose may exert neuroadaptive effects by normalizing some of the inherent molecular changes in SCZ patients, who were either medication-free or had been subjected to a lower cumulative antipsychotic medication dosage throughout life. Therefore, at least some of the differentially expressed proteins identified in L-SCZ patients may represent 'disease signatures' of SCZ as well as representing targets of antipsychotic drug action. These include effects on proteins associated with synaptogenesis, neuritic dynamics, presynaptic vesicle cycling, amino acid and glutamine metabolism, and energy buffering systems. Previously, we have identified molecular changes in proteomic (35) and metabonomic (22) studies of rats treated with antipsychotic medications. Some of these markers are altered in opposite directions to those observed in L-SCZ patients, in the present study, providing further support for our findings. For example, antipsychotics

253 affected components of the rat presynaptic vesicle machinery, neurite outgrowth dynamics and
254 synaptogenesis. Nine proteins and 2 metabolites found in these antipsychotic-treated rats were shown here to
255 be altered in L-SCZ patients (SYN2, GLUD1, GAPDH, NCAM1, ATP2B4, MAG, GNB1, GAP-43, NT, Gln
256 and Cr).
257
258 Synaptogenic alterations during the premorbid stage of illness (gestation, infancy, childhood and
259 adolescence) have been proposed in the context of the neurodevelopmental hypothesis of SCZ (48). We
260 identified alterations in key regulators of synaptogenesis (49-51) and synaptic plasticity in L-SCZ patients
261 including neurofascin1 (NFS) and tyrosine-protein phosphatase non-receptor type substrate 1 (SIRPA),
262 which have not been previously implicated in SCZ. We also identified changes in the expression of NCAM,
263 which has been reported to be altered in the brain (19, 52, 53), serum (54) and CSF (55-57) of SCZ patients.
264 Therefore, these findings support the case for synaptogenic and synaptic plasticity alterations in SCZ
265 patients (58). These findings are also supported by animal studies showing that an excess of NCAM at the
266 synapse inhibits synaptogenesis (59). The observation that NCAM was altered in all conditions examined (L-
267 SCZ, M-SCZ, H-SCZ and BPD patients) suggests that it is not affected by either antipsychotic medication or
268 mood stabilizers and that it is not specific to SCZ. Whether it is a non-specific marker of psychiatric illness
269 or a key biological change underlying brain dysfunction in both disorders requires further studies.
270
271 Prominent alterations in components involved in synaptic function have been identified by transcriptomic
272 and proteomic profiling studies of SCZ patients (16, 17, 19). Many of these findings were confirmed in our
273 study and we also identified novel changes in proteins involved in synaptic vesicle recycling/endocytosis and
274 exocytosis in the L-SCZ patients, again supporting the case for altered presynaptic vesicle cycling in SCZ.
275 Alterations in proteins involved in the synaptic endocytosis machinery such as clathrin coat assembly protein
276 AP180 (SNAP91), Hsc70 interacting protein (Hip) and reticulon1 (RTN1) have not been reported in SCZ
277 before, although synapsin 2 (SYN2) (60, 61) and another reticulon isoform (RTN4) (13, 62) have been
278 implicated previously. Though increases in syntaxin1A (STX1A) expression have been reported in SCZ (63-
279 65), we identified novel alterations in other proteins involved in presynaptic exocytosis in L-SCZ patients,
280 including a group of $G_{i/o}$ proteins (Galphai2, GNB1, GNB4, GNAO1), which are involved in the auto-
281 inhibitory feedback mechanism of exocytosis (66, 67). To our knowledge, only three recent proteomic

studies have reported increase in GNB1 expression in the PFC of patients (14, 68, 69). Significant decreases in neuronal size, number and dendritic spine density of the glutamatergic and GABAergic neurons have been observed in DLPFC (5-8) and several other brain regions (6, 70, 71) of SCZ patients. We identified alterations in a number of regulators of growth cone path finding, cell shape, structural integrity, spine dynamics and neuronal morphology. Therefore, these findings suggest a link between the aberrant levels of regulators of neuritic dynamics and the macroscopic brain pathology in SCZ. While increased neuromodulin (GAP-43) expression has been reported in the brain of SCZ patients (65, 72, 73), this is the first report showing alterations in MARCKS, Ras-related protein Rap-2A (RAP2A) and NF-M at the protein level in the DLPFC of L-SCZ patients. In addition, altered MARCKS expression in SCZ has been reported only at the transcript level (73) and NFM was found to be decreased in one study in a different brain region (anterior temporal lobe) of SCZ patients (74). Whether these changes are primary or secondary to the disease process remain to be addressed.

Elevated glutamine (Gln) levels have been reported in the DLPFC (75) and other brain regions of drug-naive and medicated SCZ patients (76-78). Our findings of increased Gln concentration and glutamate dehydrogenase expression in L-SCZ and/or M-SCZ patients are consistent with these results. Gln, or Gln-derived ammonia in excessive levels has detrimental effects on mitochondrial function since this results in excessive production of free radicals, reactive oxygen species (ROS), oxidative stress and increased neuronal nitric oxide synthase (nNOS) expression (79-81), as confirmed by Western blot analysis in this study. This suggests a possible link between Gln-induced neurotoxicity and mitochondrial dysfunction in patients (82) and is consistent with the findings from our colleagues (17) who reported mitochondrial dysfunction, energy metabolism defects and increased oxygen and ROS metabolism pathways in the DLPFC of SCZ patients.

Creatine has been found to be decreased in the anterior cingulate cortex and parieto-occipital cortices of medicated SCZ patients (83) and increased in the DLPFC (BA46) of medicated patients (21). We demonstrated that Cr was increased in the DLPFC (BA9) of L-SCZ patients and not in M-SCZ patients. Elevations in Cr concentration may be indicative of a regulatory response to increased energy turnover since at times of significant energy demand or crisis (e.g. hypoxic damage in SCZ (17)), Phospho-Cr is rapidly dephosphorylated to enable transfer of the phosphoryl group to ADP to form ATP and Cr (84). Evidence

demonstrating overexpression of creatine kinase in patients (69, 85) supports this possibility. Increased Cr levels may also reflect a neuroprotective response mechanism to mitochondrial damage and neurotoxicity (86) since it also acts as a direct anti-oxidant by scavenging ROS. Cr also regulates glycolysis, prevents reduced energy stores and improves neuronal function (87).

By identifying for the first time, that both Ala and branched amino acids (BAA's) were significantly decreased, we hypothesize that the uptake process and metabolism of these amino acids may be altered in SCZ, although future work must be conducted to confirm these findings. Reductions in these amino acids may have implications in the ammonia transport system (88), neurotransmitter synthesis (89, 90) and energy metabolism (90) given their indispensable roles in these processes.

Specificity of the changes in L-SCZ patients relative to BPD

We identified a different panel of differentially expressed membrane associated proteins in L-SCZ and BPD patients. In contrast to SCZ, BPD showed changes in a group of axon growth/branch promoting signal transduction proteins and structural proteins. These findings suggest abnormal signalling cascades regulating axon branching and cytoskeleton reorganization in BPD. This is consistent with previous studies which identified disruptions of second messenger cascades involving CAMKs and ERK/MAPK (91), abnormal G protein function and expression in brain and peripheral tissues of BPD patients (92). Increased β-tubulin expression has been found in a recent proteomic profiling study (16) and reductions in glial fibrillary acidic protein (GFAP) have also been reported in various brain regions of BPD patients (93, 94). These data demonstrate specificity of the detected changes in SCZ and BPD and suggest diverging pathological processes between the two disorders. However, as the BPD subjects were treated with mood stabilisers, effects of these drugs cannot be ruled out.

Methodological issues

The quantitative reliability of the label-free LC-MS^E proteomic profiling approach for robust identification of expression differences was demonstrated by Western blot validation of soluble and membrane fractions as well as total brain lysates. Since the corrected p-values were relatively high for the SCZ and BPD datasets

(ranging from 0.25 to 0.58), we propose a more relaxed corrected p-value cutoff threshold for brain studies using this label-free proteomic profiling platform. A microarray study conducted by Kaiser *et al.*, 2004 (95) supports this view by demonstrating that the rate of confirmation of results by RT-QPCR was 100% for genes with a corrected p-value<0.1 and 82% for genes with a corrected p-value<0.5. Although careful matching of the brain tissue samples can increase confidence of the results obtained, the realistic fact is that there are a number of additional confounders which cannot be controlled for and remain inherent caveats to these studies. These include factors such as heterogeneity and phenotypic diversity of brain tissue, possible changes in small subpopulations of brain cells, and subtle differences in the cellular distribution of proteins across different brain and cellular compartments. Schizophrenia disease subtype may also represent a source of heterogeneity. Therefore, we propose validation of results using an independent brain series although obtaining further well-characterized *post-mortem* samples from low-cumulative-medication SCZ patients remains difficult. Although we have made some progress towards distinguishing the effects of antipsychotic medication and SCZ disease signatures, there are several limitations associated with the present study. Patients were medicated differently up to the time of death and for different periods of time. In addition, since patients were treated by a mixture of typical and atypical antipsychotic drugs, the differential effects of these drugs cannot be addressed in the present study. Though we have previously addressed this effect in rat animal models (96), future studies are warranted to investigate this effect in patients. Although the effects of medication were demonstrated by comparing L-SCZ and M-SCZ patients, further confirmation of these effects by direct statistical comparison of L-SCZ and H-SCZ (matched to their own controls) patients was not possible due to their differences in the mean duration of illness. Duration of illness is an important confounding factor (97) which challenges *post-mortem* studies investigating drug naive or low-cumulative-medication patient cohorts, as these patients often have short durations of illness up to the time of death or may be in an earlier disease stage compared to chronically ill patients which live longer to receive treatments. Furthermore, patient records assume compliance in taking the prescribed medication and, compliance is known to be poor in the case of schizophrenia (98). The fluphenazine mg. equivalent is a proxy measure of drug exposure based on historical records and does not take these factors into account. Moreover, as antipsychotic medication is the mainstay of treatment for SCZ, patients who have never received medication may have additional variation distinct from those seen in medicated patients such as higher social functioning. A limitation associated with the BPD patients was that cumulative drug dosage

(antidepressants and mood stabilizers or antipsychotic drug) information for these patients is not available and thus may represent another confounding factor.

Conclusion

The present study demonstrates the utility of subproteome and metabonome profiling approaches for providing new insights into the pathophysiology and therapeutic mechanisms in schizophrenia. We found that the cumulative lifetime antipsychotic medication exerts a considerable effect on a number of proteins and metabolites in the DLPFC of patients. This suggests careful interpretation of data available to account for the confounding effects of lifetime medication levels. We identified novel protein and metabolite disease signatures of schizophrenia and targets of antipsychotic drug effects involved in synaptic connection, neuritic dynamics, presynaptic vesicle cycling, amino acid metabolism and energy buffering systems. Finally, with the exception of NCAM, we found no changes in common between SCZ and BPD, indicating the specificity of the changes and distinct pathologies. Altogether, our results may impact development of new drug discovery strategies. Furthermore, knowledge that most of the biomarkers identified are released into a variety of body fluids and peripheral tissues may facilitate translation of these markers to blood-based assays.

Acknowledgements

This research was supported by the Stanley Medical Research Institute and the donations of the Stanley brain collection courtesy of Drs. Michael B Knable, E Fuller Torrey and Robert H Yolken. Special thanks to Dr Maree Webster for providing *post-mortem* brain samples. We thank Drs. Dan Ma, Lan Wang and Xiaoping Yang for intellectual input. Many thanks to Drs. Yishai Levin and Emanuel Schwarz for LC-MS^E instrument tuning and statistical advice. Thanks to Miss Sandra Pietsch for sectioning the schizophrenia brain samples for ^1H NMR analysis. Dr. Man Chan was funded by Fundação para a Ciência e a Tecnologia, Portugal. Most of all, thanks to all patients and healthy volunteers for donating samples used in this study.

Conflict of interest

SB is Chief Scientific Officer for Psynova Neurotech Ltd. PG acts as a consultant for Psynova Neurotech Ltd. MKC, TMT, LWH, EH declare no conflict of interest.

Supplementary information is available at the Molecular Psychiatry's website.

References

1. Ferguson-Smith AC, Greally JM, Martienssen RA. The Relevance of Epigenetics to Major Psychosis. *Epigenomics*. Springer Netherlands, 2009, pp 411-434.

2. Frith C, Dolan R. The role of the prefrontal cortex in higher cognitive functions. *Brain Res Cogn Brain Res* 1996 Dec; **5**(1-2)**:** 175-181.

3. Torrey EF, Barci BM, Webster MJ, Bartko JJ, Meador-Woodruff JH, Knable MB. Neurochemical markers for schizophrenia, bipolar disorder, and major depression in postmortem brains. *Biol Psychiatry* 2005 Feb 1; **57**(3)**:** 252-260.

4. Baumann B, Bogerts B. The pathomorphology of schizophrenia and mood disorders: similarities and differences. *Schizophr Res* 1999 Sep 29; **39**(2)**:** 141-148; discussion 162.

5. Pierri JN, Volk CL, Auh S, Sampson A, Lewis DA. Decreased somal size of deep layer 3 pyramidal neurons in the prefrontal cortex of subjects with schizophrenia. *Arch Gen Psychiatry* 2001 May; **58**(5)**:** 466-473.

6. Rosoklija G, Toomayan G, Ellis SP, Keilp J, Mann JJ, Latov N *et al.* Structural abnormalities of subicular dendrites in subjects with schizophrenia and mood disorders: preliminary findings. *Arch Gen Psychiatry* 2000 Apr; **57**(4)**:** 349-356.

7. Kolluri N, Sun Z, Sampson AR, Lewis DA. Lamina-specific reductions in dendritic spine density in the prefrontal cortex of subjects with schizophrenia. *Am J Psychiatry* 2005 Jun; **162**(6)**:** 1200-1202.

8. Cotter D, Mackay D, Chana G, Beasley C, Landau S, Everall IP. Reduced neuronal size and glial cell density in area 9 of the dorsolateral prefrontal cortex in subjects with major depressive disorder. *Cereb Cortex* 2002 Apr; **12**(4)**:** 386-394.

9. Knable MB, Torrey EF, Webster MJ, Bartko JJ. Multivariate analysis of prefrontal cortical data from the Stanley Foundation Neuropathology Consortium. *Brain Res Bull* 2001 Jul 15; **55**(5)**:** 651-659.

10. Guidotti A, Auta J, Davis JM, Dong E, Grayson DR, Veldic M *et al.* GABAergic dysfunction in schizophrenia: new treatment strategies on the horizon. *Psychopharmacology (Berl)* 2005 Jul; **180**(2)**:** 191-205.

11. Beneyto M, Kristiansen LV, Oni-Orisan A, McCullumsmith RE, Meador-Woodruff JH. Abnormal glutamate receptor expression in the medial temporal lobe in schizophrenia and mood disorders. *Neuropsychopharmacology* 2007 Sep; **32**(9)**:** 1888-1902.

12. English JA, Dicker P, Focking M, Dunn MJ, Cotter DR. 2-D DIGE analysis implicates cytoskeletal abnormalities in psychiatric disease. *Proteomics* 2009 Jun; **9**(12)**:** 3368-3382.

13. Martins-de-Souza D, Gattaz WF, Schmitt A, Rewerts C, Maccarrone G, Dias-Neto E *et al.* Prefrontal cortex shotgun proteome analysis reveals altered calcium homeostasis and immune system imbalance in schizophrenia. *Eur Arch Psychiatry Clin Neurosci* 2009 Apr; **259**(3)**:** 151-163.

14. Martins-de-Souza D, Gattaz WF, Schmitt A, Maccarrone G, Hunyadi-Gulyas E, Eberlin MN *et al.* Proteomic analysis of dorsolateral prefrontal cortex indicates the involvement of cytoskeleton, oligodendrocyte, energy metabolism and new potential markers in schizophrenia. *J Psychiatr Res* 2009 Jul; **43**(11)**:** 978-986.

15. Novikova SI, He F, Cutrufello NJ, Lidow MS. Identification of protein biomarkers for schizophrenia and bipolar disorder in the postmortem prefrontal cortex using SELDI-TOF-MS ProteinChip profiling combined with MALDI-TOF-PSD-MS analysis. *Neurobiol Dis* 2006 Jul; **23**(1)**:** 61-76.

16. Pennington K, Beasley CL, Dicker P, Fagan A, English J, Pariante CM *et al.* Prominent synaptic and metabolic abnormalities revealed by proteomic analysis of the dorsolateral prefrontal cortex in schizophrenia and bipolar disorder. *Mol Psychiatry* 2007 Oct 16.

17. Prabakaran S, Swatton JE, Ryan MM, Huffaker SJ, Huang JT, Griffin JL *et al.* Mitochondrial dysfunction in schizophrenia: evidence for compromised brain metabolism and oxidative stress. *Mol Psychiatry* 2004 Jul; **9**(7)**:** 684-697, 643.

18. Smalla KH, Mikhaylova M, Sahin J, Bernstein HG, Bogerts B, Schmitt A *et al.* A comparison of the synaptic proteome in human chronic schizophrenia and rat ketamine psychosis suggest that prohibitin is involved in the synaptic pathology of schizophrenia. *Mol Psychiatry* 2008 Sep; **13**(9)**:** 878-896.

19. Behan A, Byrne C, Dunn MJ, Cagney G, Cotter DR. Proteomic analysis of membrane microdomain-associated proteins in the dorsolateral prefrontal cortex in schizophrenia and bipolar disorder reveals alterations in LAMP, STXBP1 and BASP1 protein expression. *Mol Psychiatry* 2008 Feb 12.

20. Shao L, Martin MV, Watson SJ, Schatzberg A, Akil H, Myers RM *et al.* Mitochondrial involvement in psychiatric disorders. *Ann Med* 2008; **40**(4)**:** 281-295.

21. Khaitovich P, Lockstone HE, Wayland MT, Tsang TM, Jayatilaka SD, Guo AJ *et al.* Metabolic changes in schizophrenia and human brain evolution. *Genome Biol* 2008; **9**(8)**:** R124.

22. McLoughlin G, Ma D, Tsamg TM, Jones D, Cilia J, Hill M *et al.* Analysing the Effects of Psychotropic Drugs on Metabolite Profiles in Rat Brain Using ¹H NMR Spectroscopy. *J Proteome Res* 2009 Feb 2.

23. Vawter MP, Tomita H, Meng F, Bolstad B, Li J, Evans S *et al.* Mitochondrial-related gene expression changes are sensitive to agonal-pH state: implications for brain disorders. *Mol Psychiatry* 2006 Jul; **11**(7)**:** 615, 663-679.

24. Li JZ, Vawter MP, Walsh DM, Tomita H, Evans SJ, Choudary PV *et al.* Systematic changes in gene expression in postmortem human brains associated with tissue pH and terminal medical conditions. *Hum Mol Genet* 2004 Mar 15; **13**(6)**:** 609-616.

25. Halim ND, Lipska BK, Hyde TM, Deep-Soboslay A, Saylor EM, Herman MM *et al.* Increased lactate levels and reduced pH in postmortem brains of schizophrenics: Medication confounds. *Journal of Neuroscience Methods* 2008; **169**(1)**:** 208-213.

26. Atz M, Walsh D, Cartagena P, Li J, Evans S, Choudary P *et al.* Methodological considerations for gene expression profiling of human brain. *J Neurosci Methods* 2007 Jul 30; **163**(2)**:** 295-309.

27. Cahn W, Hulshoff Pol HE, Lems EB, van Haren NE, Schnack HG, van der Linden JA *et al.* Brain volume changes in first-episode schizophrenia: a 1-year follow-up study. *Arch Gen Psychiatry* 2002 Nov; **59**(11)**:** 1002-1010.

28. Gur RE, Cowell P, Turetsky BI, Gallacher F, Cannon T, Bilker W *et al.* A follow-up magnetic resonance imaging study of schizophrenia. Relationship of neuroanatomical changes to clinical and neurobehavioral measures. *Arch Gen Psychiatry* 1998 Feb; **55**(2)**:** 145-152.

29. Berrettini W. Evidence for shared susceptibility in bipolar disorder and schizophrenia. *Am J Med Genet C Semin Med Genet* 2003 Nov 15; **123C**(1)**:** 59-64.

30. Fritzen S, Lauer M, Schmitt A, Topner T, Strobel A, Lesch KP *et al.* NO synthase-positive striatal interneurons are decreased in schizophrenia. *Eur Neuropsychopharmacol* 2007 Sep; **17**(9)**:** 595-599.

31. Lan MJ, McLoughlin GA, Griffin JL, Tsang TM, Huang JT, Yuan P *et al.* Metabonomic analysis identifies molecular changes associated with the pathophysiology and drug treatment of bipolar disorder. *Mol Psychiatry* 2009 Mar; **14**(3)**:** 269-279.

32. Abdolzade-Bavil A, Hayes S, Goretzki L, Kroger M, Anders J, Hendriks R. Convenient and versatile subcellular extraction procedure, that facilitates classical protein expression profiling and functional protein analysis. *Proteomics* 2004 May; **4**(5)**:** 1397-1405.

33. Arndt S, Poser I, Schubert T, Moser M, Bosserhoff AK. Cloning and functional characterization of a new Ski homolog, Fussel-18, specifically expressed in neuronal tissues. *Lab Invest* 2005 Nov; **85**(11)**:** 1330-1341.

34. Sabio G, Arthur JS, Kuma Y, Peggie M, Carr J, Murray-Tait V *et al.* p38gamma regulates the localisation of SAP97 in the cytoskeleton by modulating its interaction with GKAP. *EMBO J* 2005 Mar 23; **24**(6)**:** 1134-1145.

35. Ma D, Chan M, Pietsch SR, Lockstone H, Jones D, Cilia J *et al.* Antipsychotic treatment alters protein expression associated with pre-synaptic function and nervous system development in rat frontal cortex. *J Proteome Res* 2009 Apr 28.

36. Hughes MA, Silva JC, Geromanos SJ, Townsend CA. Quantitative proteomic analysis of drug-induced changes in mycobacteria. *J Proteome Res* 2006 Jan; **5**(1)**:** 54-63.

37. Silva JC, Denny R, Dorschel C, Gorenstein MV, Li GZ, Richardson K *et al.* Simultaneous qualitative and quantitative analysis of the Escherichia coli proteome: a sweet tale. *Mol Cell Proteomics* 2006 Apr; **5**(4)**:** 589-607.

38. Silva JC, Denny R, Dorschel CA, Gorenstein M, Kass IJ, Li GZ *et al.* Quantitative proteomic analysis by accurate mass retention time pairs. *Anal Chem* 2005 Apr 1; **77**(7)**:** 2187-2200.

39. Vissers JP, Langridge JI, Aerts JM. Analysis and quantification of diagnostic serum markers and protein signatures for Gaucher disease. *Mol Cell Proteomics* 2007 May; **6**(5)**:** 755-766.

40. Schwarz E, Levin Y, Wang L, Leweke FM, Bahn S. Peptide correlation: a means to identify high quality quantitative information in large-scale proteomic studies. *J Sep Sci* 2007 Sep; **30**(14)**:** 2190-2197.

41. Reiner A, Yekutieli D, Benjamini Y. Identifying differentially expressed genes using false discovery rate controlling procedures. *Bioinformatics* 2003 Feb 12; **19**(3)**:** 368-375.

42. Eriksson L, Antti H, Gottfries J, Holmes E, Johansson E, Lindgren F *et al.* Using chemometrics for navigating in the large data sets of genomics, proteomics, and metabonomics (gpm). *Anal Bioanal Chem* 2004 Oct; **380**(3)**:** 419-429.

43. Trygg J, Holmes E, Lundstedt T. Chemometrics in metabonomics. *J Proteome Res* 2007 Feb; **6**(2)**:** 469-479.

44. Hart A. Mann-Whitney test is not just a test of medians: differences in spread can be important. *BMJ* 2001 Aug 18; **323**(7309)**:** 391-393.

45. Park C, Shin KS, Ryu JH, Kang K, Kim J, Ahn H *et al.* The inhibition of nitric oxide synthase enhances PSA-NCAM expression and CREB phosphorylation in the rat hippocampus. *Neuroreport* 2004 Feb 9; **15**(2)**:** 231-234.

46. Baba H, Suzuki T, Arai H, Emson PC. Expression of nNOS and soluble guanylate cyclase in schizophrenic brain. *Neuroreport* 2004 Mar 22; **15**(4)**:** 677-680.

47. Tanda K, Nishi A, Matsuo N, Nakanishi K, Yamasaki N, Sugimoto T *et al.* Abnormal social behavior, hyperactivity, impaired remote spatial memory, and increased D1-mediated dopaminergic signaling in neuronal nitric oxide synthase knockout mice. *Mol Brain* 2009; **2**(1)**:** 19.

48. Lieberman JA, Perkins D, Belger A, Chakos M, Jarskog F, Boteva K *et al.* The early stages of schizophrenia: speculations on pathogenesis, pathophysiology, and therapeutic approaches. *Biol Psychiatry* 2001 Dec 1; **50**(11)**:** 884-897.

49. Oshima K, Ruhul Amin AR, Suzuki A, Hamaguchi M, Matsuda S. SHPS-1, a multifunctional transmembrane glycoprotein. *FEBS Lett* 2002 May 22; **519**(1-3)**:** 1-7.

50. Muller D, Mendez P, De Roo M, Klauser P, Steen S, Poglia L. Role of NCAM in Spine Dynamics and Synaptogenesis. *Neurochem Res* 2008 Mar 20.

51. Rougon G, Hobert O. New insights into the diversity and function of neuronal immunoglobulin superfamily molecules. *Annu Rev Neurosci* 2003; **26:** 207-238.

52. Vawter MP, Cannon-Spoor HE, Hemperly JJ, Hyde TM, VanderPutten DM, Kleinman JE *et al.* Abnormal expression of cell recognition molecules in schizophrenia. *Exp Neurol* 1998 Feb; **149**(2)**:** 424-432.

53. Honer WG, Falkai P, Young C, Wang T, Xie J, Bonner J *et al.* Cingulate cortex synaptic terminal proteins and neural cell adhesion molecule in schizophrenia. *Neuroscience* 1997 May; **78**(1)**:** 99-110.

54. Tanaka Y, Yoshida S, Shimada Y, Ueda H, Asai K. Alteration in serum neural cell adhesion molecule in patients of schizophrenia. *Hum Psychopharmacol* 2007 Mar; **22**(2)**:** 97-102.

55. van Kammen DP, Poltorak M, Kelley ME, Yao JK, Gurklis JA, Peters JL *et al.* Further studies of elevated cerebrospinal fluid neuronal cell adhesion molecule in schizophrenia. *Biol Psychiatry* 1998 May 1; **43**(9)**:** 680-686.

56. Poltorak M, Wright R, Hemperly JJ, Torrey EF, Issa F, Wyatt RJ *et al.* Monozygotic twins discordant for schizophrenia are discordant for N-CAM and L1 in CSF. *Brain Res* 1997 Mar 14; **751**(1)**:** 152-154.

57. Vawter MP, Usen N, Thatcher L, Ladenheim B, Zhang P, VanderPutten DM *et al.* Characterization of human cleaved N-CAM and association with schizophrenia. *Exp Neurol* 2001 Nov; **172**(1)**:** 29-46.

58. Stephan KE, Baldeweg T, Friston KJ. Synaptic plasticity and dysconnection in schizophrenia. *Biol Psychiatry* 2006 May 15; **59**(10)**:** 929-939.

59. Martin KC, Kandel ER. Cell adhesion molecules, CREB, and the formation of new synaptic connections. *Neuron* 1996 Oct; **17**(4)**:** 567-570.

60. Dyck BA, Skoblenick KJ, Castellano JM, Ki K, Thomas N, Mishra RK. Behavioral abnormalities in synapsin II knockout mice implicate a causal factor in schizophrenia. *Synapse* 2009 Apr 9; **63**(8)**:** 662-672.

61. Chen Q, He G, Qin W, Chen QY, Zhao XZ, Duan SW *et al.* Family-based association study of synapsin II and schizophrenia. *Am J Hum Genet* 2004 Nov; **75**(5)**:** 873-877.

62. Novak G, Kim D, Seeman P, Tallerico T. Schizophrenia and Nogo: elevated mRNA in cortex, and high prevalence of a homozygous CAA insert. *Brain Res Mol Brain Res* 2002 Nov 15; **107**(2)**:** 183-189.

63. Johnson RD, Oliver PL, Davies KE. SNARE proteins and schizophrenia: linking synaptic and neurodevelopmental hypotheses. *Acta Biochim Pol* 2008; **55**(4)**:** 619-628.

64. Sokolov BP, Tcherepanov AA, Haroutunian V, Davis KL. Levels of mRNAs encoding synaptic vesicle and synaptic plasma membrane proteins in the temporal cortex of elderly schizophrenic patients. *Biol Psychiatry* 2000 Aug 1; **48**(3)**:** 184-196.

65. Halim ND, Weickert CS, McClintock BW, Hyde TM, Weinberger DR, Kleinman JE *et al.* Presynaptic proteins in the prefrontal cortex of patients with schizophrenia and rats with abnormal prefrontal development. *Mol Psychiatry* 2003 Sep; **8**(9)**:** 797-810.

66. De Waard M, Hering J, Weiss N, Feltz A. How do G proteins directly control neuronal Ca2+ channel function? *Trends Pharmacol Sci* 2005 Aug; **26**(8)**:** 427-436.

67. Brown DA, Sihra TS. Presynaptic signaling by heterotrimeric G-proteins. *Handb Exp Pharmacol* 2008; (184)**:** 207-260.

68. Behan AT, Byrne C, Dunn MJ, Cagney G, Cotter DR. Proteomic analysis of membrane microdomain-associated proteins in the dorsolateral prefrontal cortex in schizophrenia and bipolar disorder reveals alterations in LAMP, STXBP1 and BASP1 protein expression. *Mol Psychiatry* 2009 Jun; **14**(6)**:** 601-613.

69. Clark D, Dedova I, Cordwell S, Matsumoto I. A proteome analysis of the anterior cingulate cortex gray matter in schizophrenia. *Mol Psychiatry* 2006 May; **11**(5)**:** 459-470, 423.

70. Roberts RC, Conley R, Kung L, Peretti FJ, Chute DJ. Reduced striatal spine size in schizophrenia: a postmortem ultrastructural study. *Neuroreport* 1996 Apr 26; **7**(6)**:** 1214-1218.

71. Harrison PJ. The neuropathology of schizophrenia. A critical review of the data and their interpretation. *Brain* 1999 Apr; **122 (Pt 4):** 593-624.

72. Perrone-Bizzozero NI, Sower AC, Bird ED, Benowitz LI, Ivins KJ, Neve RL. Levels of the growth-associated protein GAP-43 are selectively increased in association cortices in schizophrenia. *Proc Natl Acad Sci U S A* 1996 Nov 26; **93**(24)**:** 14182-14187.

73. Hakak Y, Walker JR, Li C, Wong WH, Davis KL, Buxbaum JD *et al.* Genome-wide expression analysis reveals dysregulation of myelination-related genes in chronic schizophrenia. *Proc Natl Acad Sci U S A* 2001 Apr 10; **98**(8)**:** 4746-4751.

74. Martins-de-Souza D, Gattaz WF, Schmitt A, Rewerts C, Marangoni S, Novello JC *et al.* Alterations in oligodendrocyte proteins, calcium homeostasis and new potential markers in schizophrenia anterior temporal lobe are revealed by shotgun proteome analysis. *J Neural Transm* 2009 Mar; **116**(3)**:** 275-289.

75. van Elst LT, Valerius G, Buchert M, Thiel T, Rusch N, Bubl E *et al.* Increased prefrontal and hippocampal glutamate concentration in schizophrenia: evidence from a magnetic resonance spectroscopy study. *Biol Psychiatry* 2005 Nov 1; **58**(9)**:** 724-730.

76. Bartha R, Williamson PC, Drost DJ, Malla A, Carr TJ, Cortese L *et al.* Measurement of glutamate and glutamine in the medial prefrontal cortex of never-treated schizophrenic patients and healthy controls by proton magnetic resonance spectroscopy. *Arch Gen Psychiatry* 1997 Oct; **54**(10)**:** 959-965.

77. Theberge J, Bartha R, Drost DJ, Menon RS, Malla A, Takhar J *et al.* Glutamate and glutamine measured with 4.0 T proton MRS in never-treated patients with schizophrenia and healthy volunteers. *Am J Psychiatry* 2002 Nov; **159**(11)**:** 1944-1946.

78. Theberge J, Al-Semaan Y, Williamson PC, Menon RS, Neufeld RW, Rajakumar N *et al.* Glutamate and glutamine in the anterior cingulate and thalamus of medicated patients with chronic schizophrenia and healthy comparison subjects measured with 4.0-T proton MRS. *Am J Psychiatry* 2003 Dec; **160**(12)**:** 2231-2233.

79. Lockwood AH, McDonald JM, Reiman RE, Gelbard AS, Laughlin JS, Duffy TE *et al.* The dynamics of ammonia metabolism in man. Effects of liver disease and hyperammonemia. *J Clin Invest* 1979 Mar; **63**(3)**:** 449-460.

80. Waagepetersen H, Sonnewald U, Schousboe A. Energy and Amino Acid Neurotransmitter Metabolism in Astrocytes. *Astrocytes in (Patho)Physiology of the Nervous System*. Springer US, 2009, pp 1-24.

81. Waagepetersen H, Sonnewald U, Schousboe A. Glutamine, Glutamate, and GABA: Metabolic Aspects *Handbook of Neurochemistry and Molecular Neurobiology* Springer US, 2007, pp 1-21.

82. Zoratti M, Szabo I, De Marchi U. Mitochondrial permeability transitions: how many doors to the house? *Biochim Biophys Acta* 2005 Jan 7; **1706**(1-2)**:** 40-52.

83. Ongur D, Prescot AP, Jensen JE, Cohen BM, Renshaw PF. Creatine abnormalities in schizophrenia and bipolar disorder. *Psychiatry Res* 2009 Apr 30; **172**(1)**:** 44-48.

84. Saks VA, Ventura-Clapier R, Aliev MK. Metabolic control and metabolic capacity: two aspects of creatine kinase functioning in the cells. *Biochim Biophys Acta* 1996 Jun 13; **1274**(3)**:** 81-88.

85. Martins-de-Souza D, Gattaz WF, Schmitt A, Novello JC, Marangoni S, Turck CW *et al.* Proteome analysis of schizophrenia patients Wernicke's area reveals an energy metabolism dysregulation. *BMC Psychiatry* 2009 Apr 30; **9**(1)**:** 17.

86. Terao T, Matsuda S, Kojima H, Okuno K, Hori H, Kaku A *et al.* Incidence and risk factors of benign creatine phosphokinase elevations in chronic psychiatric patients. *Neuropsychobiology* 1999 May; **39**(4)**:** 173-180.

87. Klein AM, Ferrante RJ. The Neuroprotective Role of Creatine *Creatine and Creatine Kinase in Health and Disease*, vol. 46. Springer Netherlands, 2007, pp 205-243.

88. Yudkoff M, Daikhin Y, Nissim I, Horyn O, Luhovyy B, Lazarow A. Brain amino acid requirements and toxicity: the example of leucine. *J Nutr* 2005 Jun; **135**(6 Suppl)**:** 1531S-1538S.

89. Banos G, Daniel PM, Pratt OE. The effect of age upon the entry of some amino acids into the brain, and their incorporation into cerebral protein. *Dev Med Child Neurol* 1978 Jun; **20**(3)**:** 335-346.

90. Hutson SM, Sweatt AJ, LaNoue KF. Branched Chain Amino Acids (BCAAs) in Brain. *Handbook of Neurochemistry and Molecular Neurobiology*. Springer US, 2007, pp 117-131.

91. Bezchlibnyk Y, Young LT. The neurobiology of bipolar disorder: focus on signal transduction pathways and the regulation of gene expression. *Can J Psychiatry* 2002 Mar; **47**(2)**:** 135-148.

92. Vawter MP, Freed WJ, Kleinman JE. Neuropathology of bipolar disorder. *Biol Psychiatry* 2000 Sep 15; **48**(6)**:** 486-504.

93. Johnston-Wilson NL, Sims CD, Hofmann JP, Anderson L, Shore AD, Torrey EF *et al.* Disease-specific alterations in frontal cortex brain proteins in schizophrenia, bipolar disorder, and major depressive disorder. The Stanley Neuropathology Consortium. *Mol Psychiatry* 2000 Mar; **5**(2)**:** 142-149.

94. Webster MJ, O'Grady J, Kleinman JE, Weickert CS. Glial fibrillary acidic protein mRNA levels in the cingulate cortex of individuals with depression, bipolar disorder and schizophrenia. *Neuroscience* 2005; **133**(2)**:** 453-461.

95. Kaiser S, Foltz LA, George CA, Kirkwood SC, Bemis KG, Lin X *et al.* Phencyclidine-induced changes in rat cortical gene expression identified by microarray analysis: implications for schizophrenia. *Neurobiol Dis* 2004 Jun; **16**(1)**:** 220-235.

96. Ma D, Chan MK, Lockstone HE, Pietsch SR, Jones DN, Cilia J *et al.* Antipsychotic treatment alters protein expression associated with presynaptic function and nervous system development in rat frontal cortex. *J Proteome Res* 2009 Jul; **8**(7)**:** 3284-3297.

97. Velakoulis D, Wood SJ, Smith DJ, Soulsby B, Brewer W, Leeton L *et al.* Increased duration of illness is associated with reduced volume in right medial temporal/anterior cingulate grey matter in patients with chronic schizophrenia. *Schizophr Res* 2002 Sep 1; **57**(1)**:** 43-49.

98. McIntosh AM, Conlon L, Lawrie SM, Stanfield AC. Compliance therapy for schizophrenia. *Cochrane Database Syst Rev* 2006; **3:** CD003442.

99. Honer WG, Falkai P, Bayer TA, Xie J, Hu L, Li HY *et al.* Abnormalities of SNARE mechanism proteins in anterior frontal cortex in severe mental illness. *Cereb Cortex* 2002 Apr; **12**(4)**:** 349-356.

100. Gabriel SM, Haroutunian V, Powchik P, Honer WG, Davidson M, Davies P *et al.* Increased concentrations of presynaptic proteins in the cingulate cortex of subjects with schizophrenia. *Arch Gen Psychiatry* 1997 Jun; **54**(6)**:** 559-566.

101. Arion D, Unger T, Lewis DA, Levitt P, Mirnics K. Molecular evidence for increased expression of genes related to immune and chaperone function in the prefrontal cortex in schizophrenia. *Biol Psychiatry* 2007 Oct 1; **62**(7)**:** 711-721.

102. Pennington K, Beasley CL, Dicker P, Fagan A, English J, Pariante CM *et al.* Prominent synaptic and metabolic abnormalities revealed by proteomic analysis of the dorsolateral prefrontal cortex in schizophrenia and bipolar disorder. *Mol Psychiatry* 2008 Dec; **13**(12)**:** 1102-1117.

103. Narayan S, Tang B, Head SR, Gilmartin TJ, Sutcliffe JG, Dean B *et al.* Molecular profiles of schizophrenia in the CNS at different stages of illness. *Brain Res* 2008 Aug 16.

104. Tkachev D, Mimmack ML, Ryan MM, Wayland M, Freeman T, Jones PB *et al.* Oligodendrocyte dysfunction in schizophrenia and bipolar disorder. *Lancet* 2003 Sep 6; **362**(9386)**:** 798-805.

Tables

Table 1. Summary of patient demographics and procedural features of each study group (mean±SD, ranges in parenthesis). a) Summary of demographic details for L-SCZ and M-SCZ subjects and, BPD patients and CT subjects (used for LC-MS^E, ^{1}H NMR spectroscopy and Western blot validation). **b)** Summary of demographic details for H-SCZ and CT subjects (used for Western blot validation only).

					p-values obtained by T-test or *Fisher's exact test			
a)	**L-SCZ (n=10)**	**M-SCZ (n=10)**	**BPD (n=10)**	**CT (n=10)**	**L-SCZ versus CT**	**M-SCZ versus CT**	**BPD versus CT**	**L-SCZ versus M-SCZ**
Age of onset	23.60±5.58 (15-33)	22.90±5.74 (16-34)	28.50±11.38 (17-48)	—	—	—	—	0.79
Age of death	38±12.90 (19-57)	43.1±6.38 (31-54)	44.30±9.68 (29-59)	42.4±6.29 (34-52)	0.35	0.81	0.61	0.28
Duration of illness (years)	14.42±13.75 (0.2-37)	20.20±8.12 (5-31)	15.80±6.53 (9-29)	—	—	—	—	0.27
PMI (hours)	27.80±10.43 (13-48)	39.20±21.19 (9-80)	41.90±18.90 (18-70)	31.90±14.42 (11-52)	0.48	0.38	0.2	0.15
Brain pH	6.54±0.20 (6.20-6.80)	6.44±0.23 (6.20-6.80)	6.60±0.20 (6.20-6.90)	6.42±0.26 (6.00-6.70)	0.27	0.86	0.10	0.33
Gender (M/F)	6/4	8/2	6/4	7/3	*1.00	*1.00	*1.00	*0.63
FME	6515±6465 (0-15000)	86200±47499 (34000-180000)	N/A	—	—	—	—	0.0005
SCZ subtype (Undifferentiated/ Schizophreniform disorder/Paranoid/ Disorganized)	9/1/0/0	6/0/4/0	—	—	N/A	N/A	N/A	*0.30

			p-values obtained by T-test or *Fisher's exact test
b)	**H-SCZ (n=10)**	**CT (n=10)**	**H-SCZ versus CT**
Age of onset	20.20±3.85 (14-28)	—	—
Age of death	47.30±6.40 (35-54)	46.50±7.63 (34-59)	0.80
Duration of illness (years)	27.10±5.32 (20-37)	—	—
PMI (hours)	27.00±15.14 (9-47)	29.60±11.27 (13-47)	0.67
Brain pH	6.32±0.24 (5.90-6.70)	6.71±0.13 (6.5-6.9)	0.0005
Gender (M/F)	9/1	9/1	*1.00
FME	182500±123855 (60000-400000)	—	—
SCZ subtype (Undifferentiated/ Schizophreniform disorder/ Paranoid/Disorganized)	8/0/1/1	N/A	—

Key: L-SCZ: low-cumulative-medication schizophrenia patients (drug-naive or low cumulative lifetime antipsychotic medication; FME=0-15000); **M-SCZ:** medium-cumulative-medication schizophrenia patients (FME=34000-180000); **BPD:** bipolar disorder patients who received mood stabilisers and antidepressants, plus brief antipsychotic treatment (FME not calculated); **CT:** control or non-psychotic healthy individuals. **FME:** Fluphenazine mg. equivalents (cumulative lifetime antipsychotic medication dose). **H-SCZ:** high-cumulative-medication schizophrenia patients (FME=60000-400000).

742 **Table 2. Differentially expressed proteins identified in L-SCZ patients**

Gene name	UniprotKB accession	Protein name	*p*-value	Corrected *p*-value	FC (fold change)	Described in DLPFC of SCZ (*=transcriptomic and #=proteomic profiling/assay)
Cell communication / signal transduction						
▼ST13	P50502	Hsc70-interacting protein (Hip)	0.03	0.58	-1.32	----------
▲Q6B6N3	Q6B6N3	Galphai2 protein	0.05	0.58	1.15	----------
▲NCAM1	P13591	Neural cell adhesion molecule 1 (140 kDa)	0.03	0.58	1.14	▲#(19), ▲#(52), ▲ #(53)
▲NFASC	O94856	Neurofascin	0.05	0.58	1.16	----------
▲GNB1	P62873	Guanine nucleotide-binding protein subunit beta-1	0.05	0.58	1.17	▲#(14), ▲#(68), ▲#(69)
▲RTN1	Q16799	Reticulon-1	0.03	0.58	1.18	▲*(73)
▲SIRPA	P78324	Tyrosine-protein phosphatase non-receptor type substrate 1	0.02	0.58	1.20	▼#(13)
▲SNAP91	O60641	Clathrin coat assembly protein AP180	0.02	0.58	1.21	----------
▲RAP2A	P10114	Ras-related protein Rap-2a precursor	0.03	0.58	1.21	----------
▲STX1A	Q16623	Syntaxin-1A	0.04	0.58	1.24	▲#(53), ▲#(99), ▲#(100), ▲*(64)
▲OPA1	O60313	Dynamin-like 120 kDa protein	0.03	0.58	1.25	▲#(13)
▲SYN2	Q92777	Synapsin-2	0.04	0.58	1.26	▼*(101)
▲GAP43	P17677	Neuromodulin	0.04	0.58	1.27	▲#(72),▲*(73)
▲GNB4	Q9HAV0	Guanine nucleotide-binding protein subunit beta-4	0.01	0.58	1.28	----------
▲GNAO1	P09471	Guanine nucleotide-binding protein G(o) subunit alpha	0.05	0.58	1.30	----------
Cell growth and/or maintenance						
▼NEFM	P07197	Neurofilament medium polypeptide (NF-M)	0.02	0.58	-2.06	▼#(74), ▼# (102)
▲MARCKS	P29966	Myristoylated alanine-rich C-kinase substrate	0.00	0.58	1.51	▲*(73)
Immune response						
▼MAG	P20916	Myelin-associated glycoprotein precursor	0.05	0.58	-2.35	▼*(73), ▼*(103), ▼*(104)
▼SCRN1	Q12765	Secernin-1	0.03	0.58	-1.21	▲#(102)
Metabolism / energy pathways						
▼PADI2	Q9Y2J8	Protein-arginine deiminase type-2	0.03	0.58	-1.28	----------
▼GAPDH	P04406	Glyceraldehyde-3-phosphate dehydrogenase (EC 1.2.1.12)	0.02	0.58	-1.24	▼#(17), ▲#(13)
▼PRDX6	P30041	Peroxiredoxin-6	0.03	0.58	-1.20	▲#(13),
▲GLUD1	P00367	Glutamate dehydrogenase 1 (EC 1.4.1.3)	0.02	0.58	1.19	----------
▼GAPD	Q5ZEY3	Glyceraldehyde-3-phosphate dehydrogenase	0.02	0.58	-1.13	----------
▲PDHA1	Q5JPT8	Pyruvate dehydrogenase	0.02	0.58	1.25	----------
▼HSP90AA1	P07900	Heat shock protein HSP 90-alpha	0.02	0.58	-1.16	▼#(14)
Transport						
▼Q8TCR7	Q8TCR7	Putative uncharacterized protein DKFZp761K0922	0.02	0.58	-1.95	----------
▲ATP2B4	P23634	Plasma membrane calcium-transporting ATPase 4	0.04	0.58	1.12	▲#(74)
▲AQP4	Q6L7A0	Aquaporin type4 transcript variant c	0.04	0.58	1.70	----------
Biological process unknown						
▲NTM	Q9P121	Neurotrimin	0.03	0.58	1.30	----------
▲GDAP1	Q8TB36	Ganglioside-induced differentiation-associated protein 1	0.04	0.58	1.30	----------
▲SH3GL2	Q3V638	SH3-domaingrb2-like2	0.05	0.58	1.22	▲#(13), ▼#(17)
Neurogenesis						
▲GPM6A	P51674	Neuronal membrane glycoprotein M6-a	0.05	0.58	1.27	----------
Response to biotic stimulus						
▲PRRT2	Q7Z6L0	Proline-rich transmembrane protein 2	0.01	0.58	1.34	----------

743

744

745

746

747

748

749

Figures

Figure 1. Distinct biological processes in L-SCZ and BPD

Figure 2. a) Validation of proteomic profiling results in *post-mortem* DLPFC from L-SCZ subjects. Representative Western blot images with numbers in parentheses indicating fold changes; significance at **p*<0.05 and ***p*<0.01. Antibodies used (Abcam; Cambridge, UK, unless otherwise stated): N-CAM (1:6000; BD Biosciences, Oxford, UK), MARCKS (1:7000), GAP43 (1:2000), nNOS (1:7000), NFM (1:10000), MAG (1:1000), Calmodulin (1:5000; loading control), β-tubulin III (1:20000). **b) Quantitative summary of Western blot validation results.**

Figure 3. a) Multivariate analysis of ^{1}H NMR spectra generated from *post-mortem* brain extracts. Plots on the left show the separation for the PLS-DA scores for **A)** L-SCZ vs control and **B)** M-SCZ vs control. Plots on the right **C)** and **D)** represent the corresponding O-PLS-DA loading coefficient plots, showing spectral descriptors which distinguish the disease from the control groups. Direction of change is indicated by signal orientation (positive values indicate spectral regions co-varying with disease while negative correlation values specify spectral regions co-varying with controls). The range of spectral colour is proportional to the strength of the correlation with disease (red indicates highest correlation and blue indicates no correlation) based on R^2 values. **b) List of metabolite changes in schizophrenia.** Numbers in parentheses indicate fold changes; significance at **p*<0.05 and ***p*<0.01.

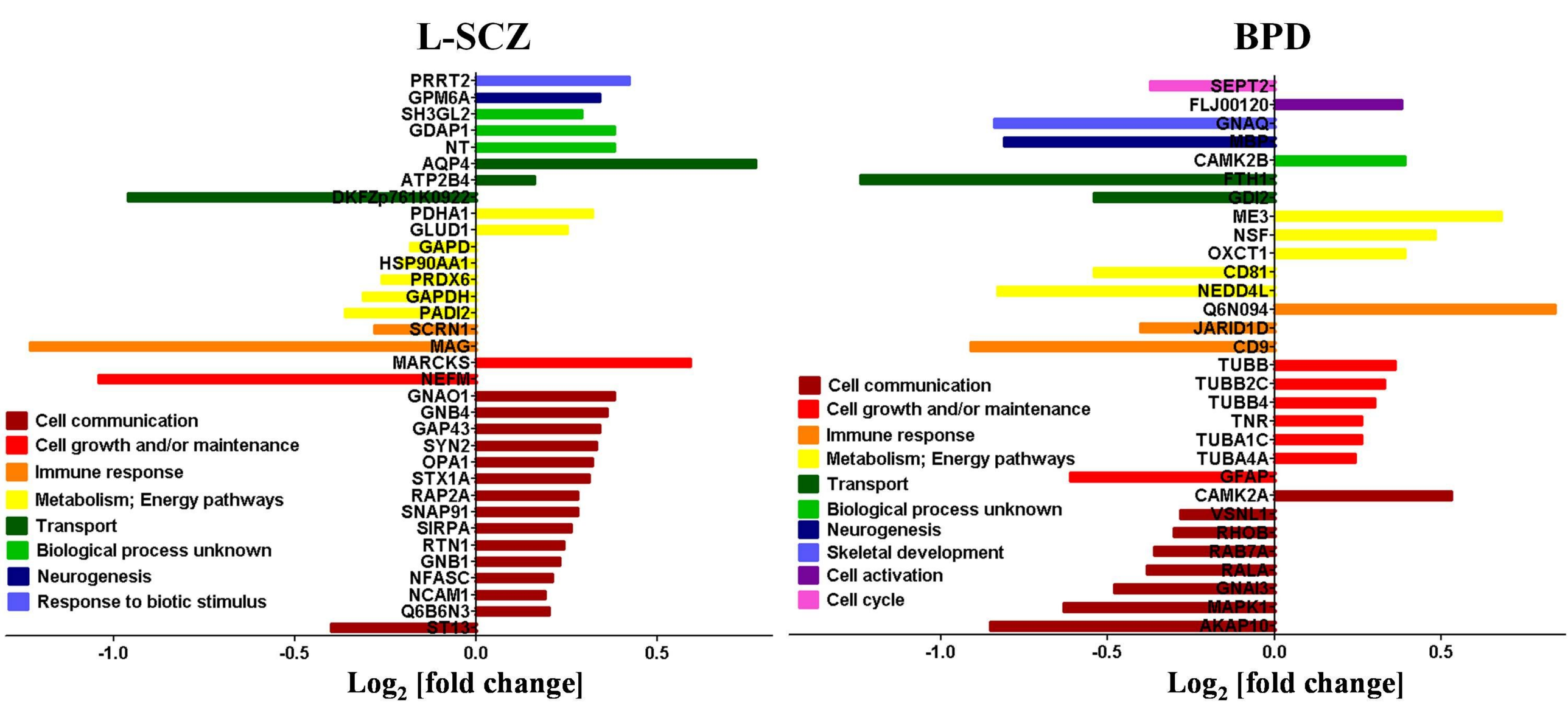
L-SCZ
PRRT2
GPM6A
SH3GL2
GDAP1
NT
AQP4
ATP2B4
DKFZp761K0922
PDHA1
GLUD1
GAPD
HSP90AA1
PRDX6
GAPDH
PADI2
SCRN1
MAG
MARCKS
NEFM
GNAO1
GNB4
GAP43
SYN2
OPA1
STX1A
RAP2A
SNAP91
SIRPA
RTN1
GNB1
NFASC
NCAM1
Q6B6N3
ST13
Cell communication
Cell growth and/or maintenance
Immune response
Metabolism; Energy pathways
Transport
Biological process unknown
Neurogenesis
Response to biotic stimulus
-1.0
-0.5
0.0
0.5
Log2 [fold change]
BPD
SEPT2
FLJ00120
GNAQ
MBP
CAMK2B
FTH1
GDI2
ME3
NSF
OXCT1
CD81
NEDD4L
Q6N094
JARID1D
CD9
TUBB
TUBB2C
TUBB4
TNR
TUBA1C
TUBA4A
GFAP
CAMK2A
VSNL1
RHOB
RAB7A
RALA
GNAI3
MAPK1
AKAP10
Cell communication
Cell growth and/or maintenance
Immune response
Metabolism; Energy pathways
Transport
Biological process unknown
Neurogenesis
Skeletal development
Cell activation
Cell cycle
-1.0
-0.5
0.0
0.5
Log2 [fold change]

a)

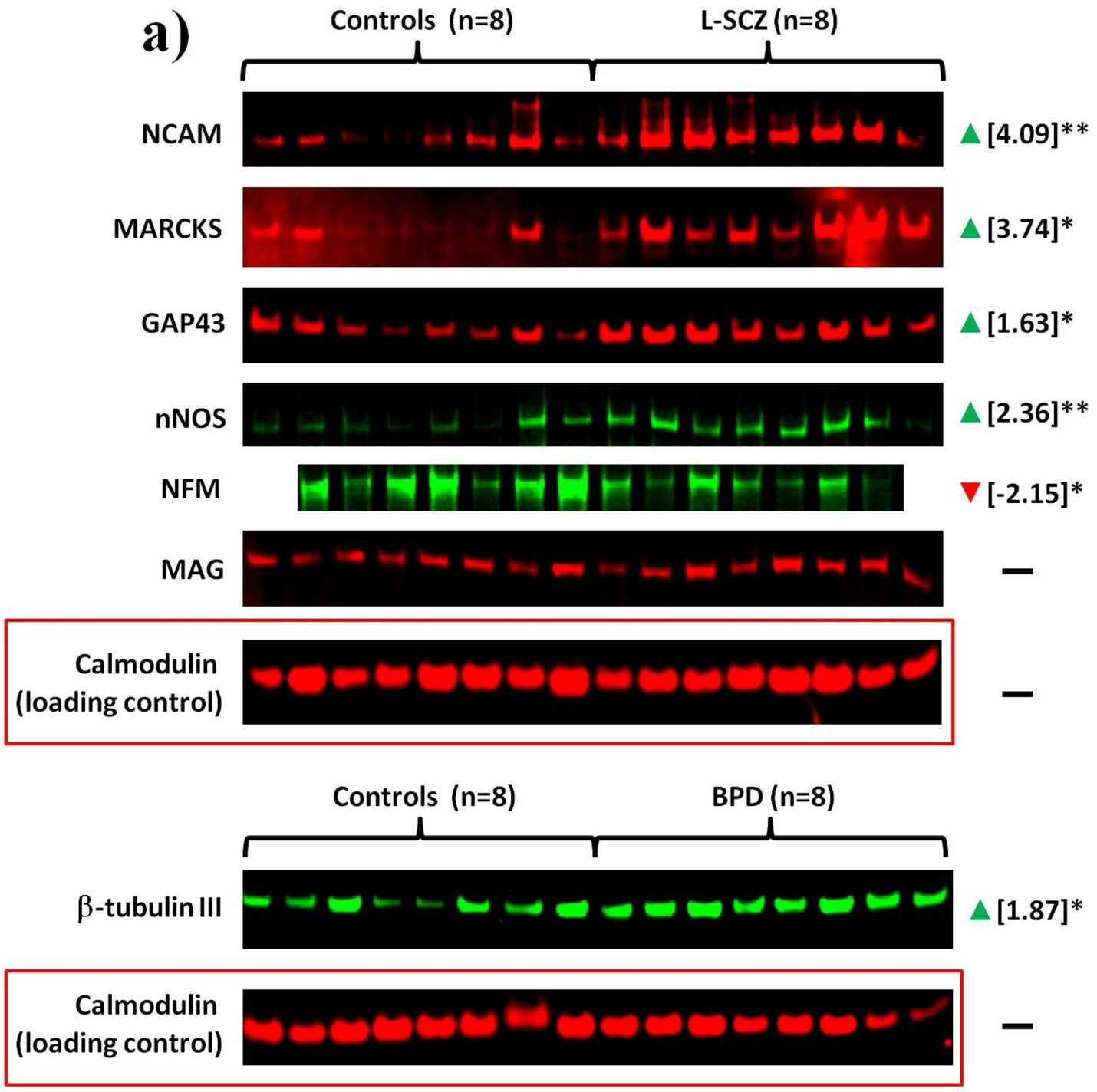

b)

Candidate protein	L-SCZ versus control								M-SCZ versus control		H-SCZ versus control		BPD versus control			
	LC-MS^E		Western blot		Western blot				Western blot		Western blot		LC-MS^E		Western blot	
	Membrane fractions				Soluble fractions		Total brain lysates		Membrane fractions		Membrane fractions		Membrane fractions			
	p-value	FC	p-value	FC	p-value	FC	p-value	FC	p-value	FC	p-value	FC	p-value	FC	p-value	FC
MARCKS	▲ 0.003	1.51	▲ 0.010	3.74	▲ 0.030	2.42	▲ 0.040	1.58	— 0.400	1.57	— 0.180	-1.26	— 0.590	1.07	— 0.240	1.57
nNOS	▲ predicted		▲ 0.009	2.36	▲ 0.040	1.73	▲ 0.027	1.95	— 0.190	1.69	— 0.370	-1.29	N/A		— 0.210	1.58
NCAM	▲ 0.030	1.14	▲ 0.007	4.09	undetected		▲ 0.040	2.30	▲ 0.010	2.95	▲ 0.030	1.78	— 0.880	-1.02	▲ 0.030	1.78
GAP43	▲ 0.038	1.27	▲ 0.010	1.63	▲ 0.020	1.41	— 0.190	1.43	— 0.720	1.06	— 0.900	-1.01	— 0.240	1.13	— 0.790	1.07
MAG	▼ 0.045	-2.35	— 0.150	1.15	— 0.860	1.00	— 0.070	1.34	— 0.930	1.00	— 0.110	-1.34	— 0.200	-1.84	— 0.430	1.06
NFM	▼ 0.020	-2.06	▼ 0.045	-2.15	▼ 0.045	-3.03	— 0.800	-1.12	— 0.250	1.50	▼ 0.040	-3.34	— 0.800	-1.17	IS	
CALM	— 0.750	-1.10	— 0.340	1.12	— 0.720	1.00	— 0.190	-1.17	— 0.590	-1.08	— 0.080	1.19	— 0.280	1.16	— 0.710	1.00
β-TUB	----------		----------		----------		----------		----------		----------		▲ 0.010	1.28	▲ 0.010	1.87

IS: insufficient samples

a)

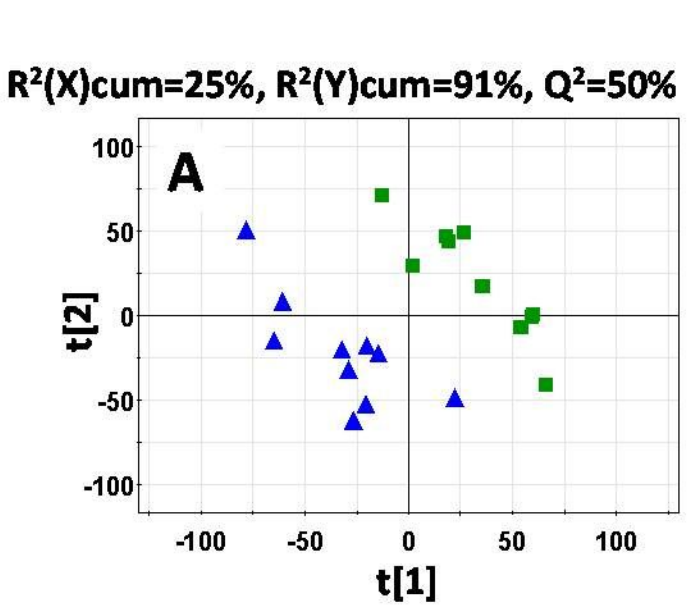

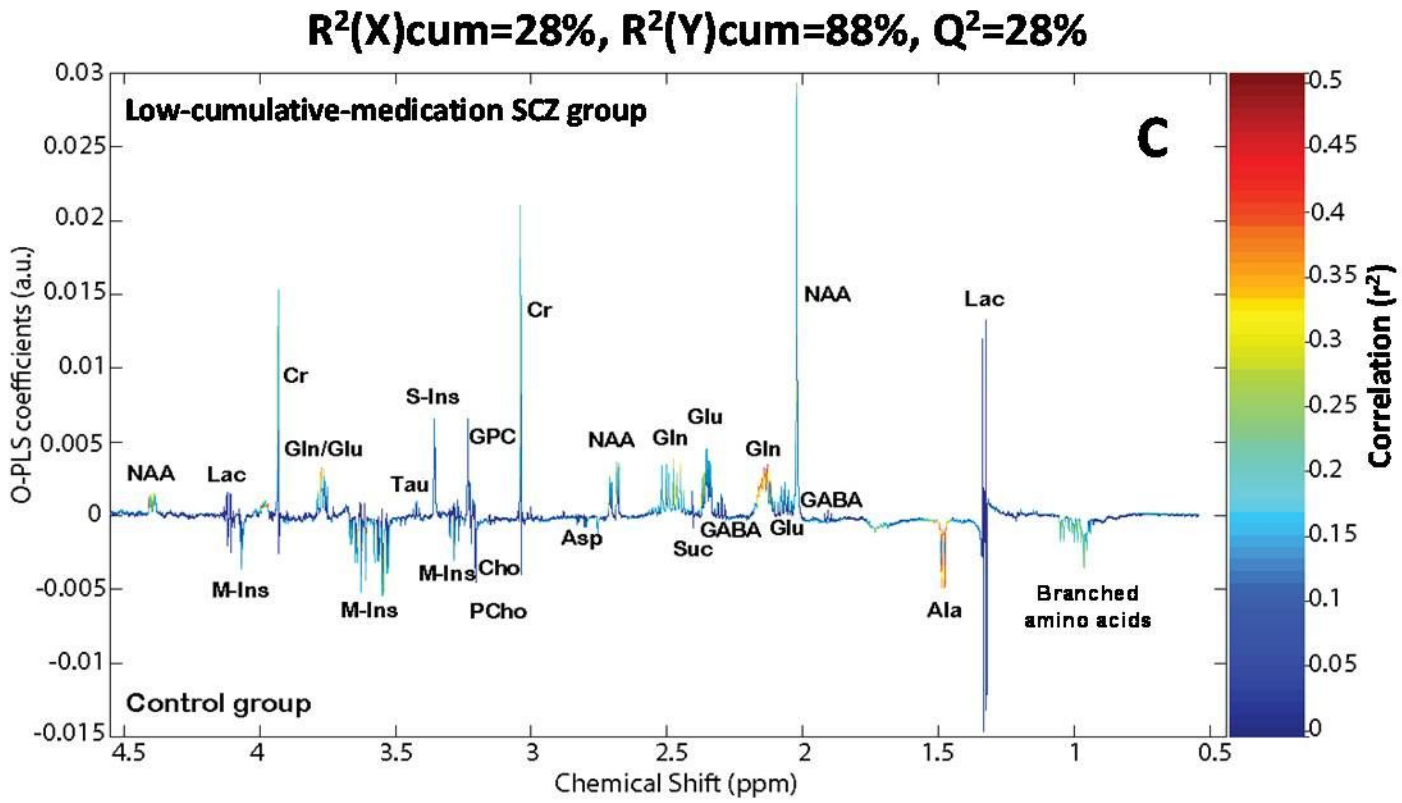

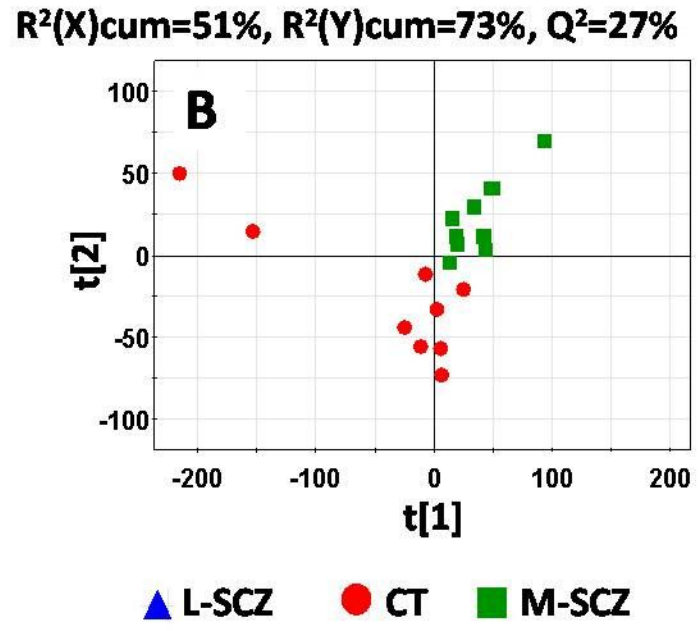

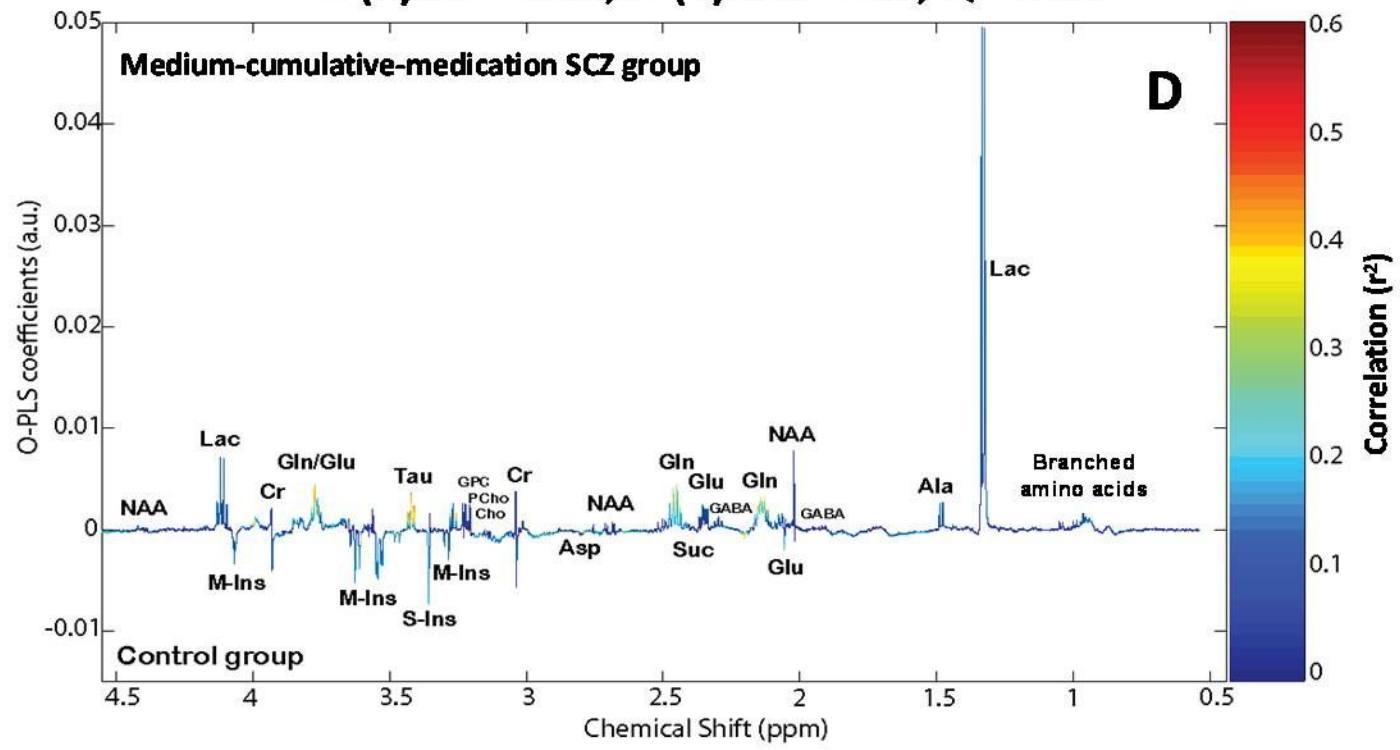

b)

Metabolites	L-SCZ versus Control	M-SCZ versus Control
Branched amino acids	▼ [-1.28]*	—
Lactate	—	—
Alanine	▼ [-1.22]**	—
GABA	—	—
NAA	—	—
Glutamate	—	—
Glutamine	▲ [1.14]**	▲ [1.11]*
Aspartate	—	—
Succinate	—	—
Creatine	▲ [1.11]*	—
Choline	—	—
Phophocholine	—	—
GPC	—	—
Myo-inositol	—	—
Taurine	—	▲ [1.24]**
Scyllo-inositol	—	—